Available online at www.sciencedirect.com
ScienceDirect
Optics Communications 281 (2008) 2424–2428
OPTICS COMMUNICATIONS
www.elsevier.com/locate/optcom

The application of MUSIC algorithm in spectrum reconstruction and interferogram processing

Xiaohua Jian [a], Chunmin Zhang [a,*], Baochang Zhao [b], Baohui Zhu [a]

[a] School of Science, Xi'an Jiao Tong University, Xi'an 710049, PR China
[b] Xi'an Institute of Optics and Precision Mechanics, Academia Sinica, Xi'an 710068, PR China

Received 26 August 2007; received in revised form 17 December 2007; accepted 18 December 2007

Abstract

Three different methods of spectrum reproduction and interferogram processing are discussed and contrasted in this paper. Especially, the nonparametric model of MUSIC (multiple signal classification) algorithm is firstly brought into the practical spectrum reconstruction processing. The experimental results prove that this method has immensely improved the resolution of reproduced spectrum, and provided a better math model for super advanced resolving power in spectrum reconstruction. The usefulness and simplicity of the technique will lead the interference imaging spectrometers to almost every field into which the spectroscopy has ventured and into some where it has not gone before.

Keywords: Spectrum reconstruction; MUSIC algorithm; Polarization interference imaging spectrometer

1. Introduction

The technique of interference imaging spectrometers developing fast in the 1980's was pioneered by Michelson in 1891. The advantages of these spectrometers arise from two major concepts known as the Fellgett and Jacquinot advantages. Several additional advantages follow them and can be listed as follows: large resolving power; high wave number accuracy; fast scanning time; smaller size, lower weight and so on. Because of these, now governments, armies and many international imaging spectrum organizations all around the world spend much more attention on the interference spectrometers which could be widely used in many different fields. There have been major typical spectrometers such as those: the spatial interference imaging spectrometers based on the Sagnac spectroscope by Florida Tech, USA in 1995 [1]; the Digital array scanned interferometer based on birefringent crystal by University of Washington, in 1992 [2]; the spatial spectrometer based on Wollaston prism by University of San Francisco in 1995 [3] and the spatial and time modulated interferometer imaging spectrometer based on the Savart Plat, by CM Zhang, BC Zhao, LB Xiang et al. in 2000 [4–8].

Although there are great varieties of spectrometers currently, the work of spectrum reconstruction and interferogram processing is always necessary and important, without which the useful information about the detected objects can not be obtained. This work also determines the applied field and performance of the spectrometers. But the traditional reproduction technique is complex and the resolving power is lower and limited that can not meet the need of study and work. Therefore, the MUSIC algorithm which is maturely used in power spectrum estimation is introduced into the spectrum reconstruction processing for the first time and a better and higher resolving power is achieved [9]. The particular process and principle of this method would be described in Section 5 of this paper.

* Corresponding author.
E-mail address: zcm@mail.xjtu.edu.cn (C. Zhang).

0030-4018/$ - see front matter © 2007 Elsevier B.V. All rights reserved.
doi:10.1016/j.optcom.2007.12.050

2. Principles

Fig. 1 shows the optical diagram of the PIIS (polarization interference imaging spectrometer) [4,10–12]. It consists of pre-telescope system, polarized interferometer (polarizer P1, Savart polariscope and analyzer P2), imaging lens, detector and the system of acquiring and processing signals. The key component in the spectrometer is a Savart polariscope. The Savart polariscope consists of two identical uniaxial crystals that are cut so that their optical axes are aligned at 45° to the optical axis of the system. The optical axis of the second crystal is perpendicular to the first one (we use two identical plates with their principal section crossed). In the first crystal the incident beams are divided into two components, the ordinary ray and the extraordinary ray. The ordinary ray satisfies Snell's law while the extraordinary one does not. As a result the extraordinary ray deviates from the ordinary one. Because the optic axis of the second crystal is perpendicular to the first one, the ordinary ray in the first crystal changes to the extraordinary ray, while the extraordinary ray changes to the ordinary one. The output rays are parallel laterally sheared but not longitudinally sheared. As a result the Savart polariscope splits the source into two virtual sources.

It is clear that narrow slit in dispersive device and DASI or spatially modulated interference imaging spectrometer can be replaced by the field view stop in PIIS. Parallel light is polarized by linear polarizer P1 and is split into two polarized components by Savart polariscope. The Savart polariscope shears the two components laterally and the analyzer P2 is used to make two components interfere. The lens is employed to image the fringes onto detector. Interferogram and target's image in the spatial domain are recorded by 2D detector.

As is known from Fourier transform spectroscopy [13], the rationale underlying the analysis of the PIIS may be simply stated. The interference intensity of the interferogram is

$$I(\Delta) = \int_{-\infty}^{+\infty} B(\sigma) e^{i2\pi\sigma\Delta} d\sigma \quad (1)$$

where I is the interferogram, B is the spectrum, Δ is the path difference and σ is the wave number. The reconstructed spectrum of the input light is

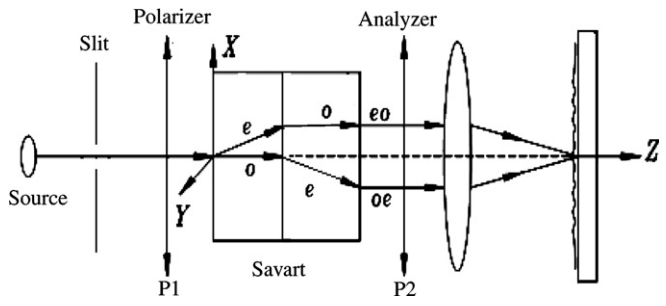

Fig. 1. Optical diagram of the PIIS based on a Savart plate birefringent interferometer.

$$B(\sigma) = \int_{-\infty}^{+\infty} I(\Delta) e^{-i2\pi\sigma\Delta} d\Delta \quad (2)$$

Function (1), and (2) is the most important relationship of spectrum and interferogram, also the basis of the interference imaging spectroscopy.

3. The spatial modulation

The spatially modulated polarization interference imaging spectrometer using an array CCD(detector) without moving parts could get information about a line detected object in scanning field at one time, while the time modulated ones have to move a periodic time for getting necessary interferogram. When it is scanning, each point's interferogram of the detected target is recorded in the corresponding line of the CCD, and the whole array CCD is filled with a line point's interferogram of the detected object [14–17]. So while it is scanning the detected field, the whole interferogram of the range is recorded. It is very easy to collect and operate the interferogram in time using this modulation, which is widely used in both experiments and practices.

4. Interferogram preprocessing

Fig. 2a shows monochromatic light source's (He–Ne laser, $\lambda = 632.8$ nm) interferograms and images which are collected by our designed spatially modulated polarization interference imaging spectrometer in the space-borne simulation experiment. The regime of signal to noise (SNR) ratio of this image is about 200–250, and more detailed description of SNR of the PIIS can be found in [18]. Fig. 2b shows the result (one point whose interferential data are selected by the spatial modulation, satisfying the sampling theorem) after the wave filtering and background processing on (a).

5. Spectrum reproduction

After necessary processing just like apodization and phase correction [13], the spectrums are ready to be reconstructed according to the basic Fourier transform spectroscopy integrals (1) and (2). The reconstructed spectrums by different ways and the analysis and comparison about the results are shown below:

5.1. FFT

Fig. 3 shows the reconstructed transmittance spectrum (power spectrum) of the quasi-monochromatic light, which is obtained through fast Fourier transform (FFT) from a two-sided sampling interferogram with an apodization by a triangle function in Fig. 2b.

The profile of the reconstructed spectrum is in approximate agreement with the original spectrum as shown in Fig. 3, but badly extending and having lots of side-lobes

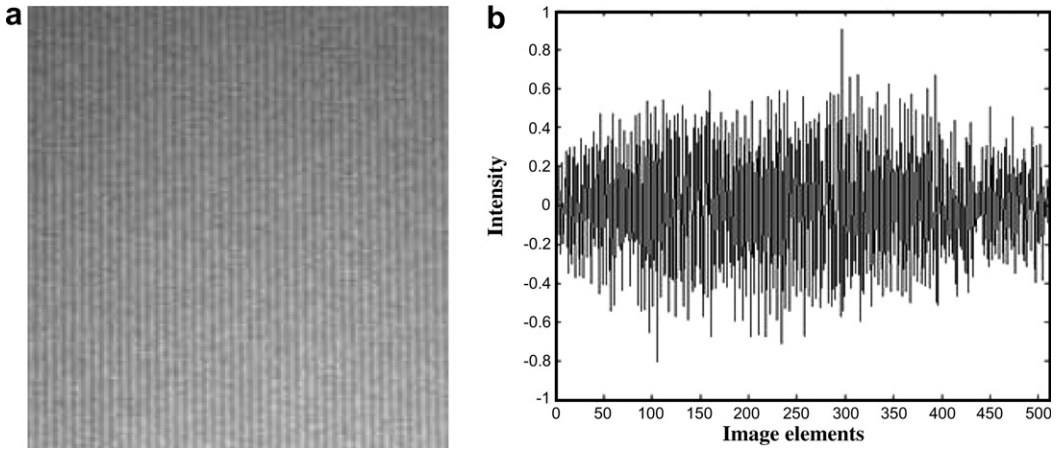

Fig. 2. (a) Interferogram and image of monochromatic light source and (b) interferential data (one point of detected target) obtained by wave filtering and background processing.

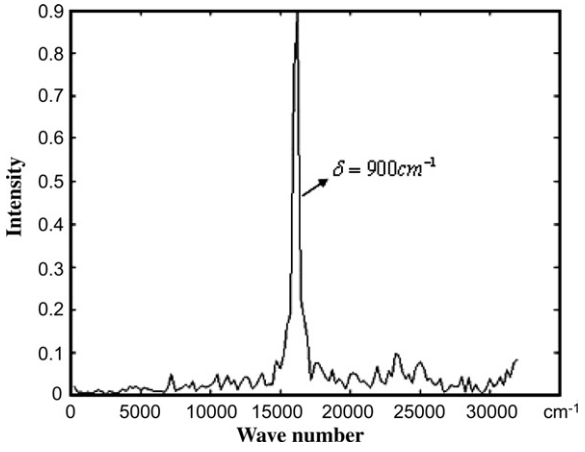

Fig. 3. Reconstructed transmittance spectrum of quasi-monochromatic light by FFT.

which would destructively disturb the resolution power and the accuracy. Especially in the spectrum of polychromatic light, the side-lobes would easily generate false peaks and this might distort the reconstructed spectrum. The FWHM (full wave at half maximum) is almost 900 cm^{-1}, the resolving power is about 20 nm according to the Rayleigh criterion.

The amendatory spectrum may be got if the spectrum is on an average by reconstructing fragments and parts of the interferogram with overlapping. But the overlapping extent must be carefully chosen: if it is too much, the spectrum will be distorted; too little, the improvement will be neglectable. And it is very difficult to decide the concrete overlapping unit, so the modern power spectrum estimation is accepted. Specially, the nonparametric model of MUSIC algorithm which is maturely used in power spectrum estimation prodigiously improved the resolution of reproduced spectrum, and provided a better math model and the possibility of improvement for super advanced resolving power in spectrum reproduction. It will be described in detail in Section 5.3.

5.2. Parametric model – autoregression (AR)

Since the interferogram can not be scanned to infinity like theoretical calculation, but from $\Delta = -L$ to $\Delta = +L$ (L is the maximum path difference). In Fourier transform spectroscopy these interferogram value, out of scanning range, is considered as zero. This is called apparatus function that limits the resolving power just like a window (rectangular) function. Meanwhile, the basic idea of modern power spectrum estimation is to found an appropriate math model to estimate the interferogram rational value out of scanning range instead of zeros.

Autoregression (AR) is a full-pole model, the three basic relational expressions are shown below as functions (3)–(5)

$$x(n) = -\sum_{k=1}^{p} a_k x(n-k) + u(n) \tag{3}$$

$$H(z) = \frac{1}{A(z)} = \frac{1}{1 + \sum_{k=1}^{p} a_k z^{-k}} \tag{4}$$

$$P_x(e^{j\omega}) = \frac{\sigma^2}{\left|1 + \sum_{k=1}^{p} a_k e^{-j\omega k}\right|^2} \tag{5}$$

where $x(n)$ is the interferogram, a_k is the model parameter, $|H(z)|$ is the transfer function, $P_x(e^{j\omega})$ is the spectrum, σ^2 is the variance of $x(n)$. Because the canonical equation of AR is a linear system of equations, it is easy to derivate, the AR model is the mostly used model. The canonical equation expresses the relationship of autocorrelation function about a_k and $x(n)$. Eq. (6) is its matrix expression.

$$\begin{bmatrix} r_x(0) & r_x(1) & r_x(2) & \cdots & r_x(p) \\ r_x(1) & r_x(0) & r_x(1) & \cdots & r_x(p-1) \\ r_x(2) & r_x(1) & r_x(0) & \cdots & r_x(p-2) \\ \vdots & \vdots & \vdots & & \vdots \\ r_x(p) & r_x(p-1) & r_x(p-2) & \cdots & r_x(0) \end{bmatrix} \begin{bmatrix} 1 \\ a_1 \\ a_2 \\ \vdots \\ a_p \end{bmatrix} = \begin{bmatrix} \sigma^2 \\ 0 \\ 0 \\ \vdots \\ 0 \end{bmatrix} \tag{6}$$

There are $p+1$ model parameters in a p hierarchy AR, just like $a_1,\ldots,a_p,\sigma^2$. If $r_x(0)$,$r_x(1)$,... and $r_x(p)$ are known, the front p autocorrelation functions about $x(n)$, the model parameters will be got. The parameter matrix is Toeplitz-Matrix, which could be solved using Levinson–Durbin integration by successive reductions.

Although the autocorrelation function is a finite sequence, the modern power spectrum estimation implies the extrapolation of data and their autocorrelation functions. It means more data are used to reconstruct the spectrum, and then the resolving power is improved. Fig. 4 shows the reconstructed transmittance spectrum of the quasi-monochromatic light, which is obtained through AR model, fewer side lobes, the FWHM is about 250 cm^{-1}, whose resolving power is nearly double of FFT's. But at the same time the work of computation is doubled too. And choosing a suitable hierarchy number is a very important and difficult thing for AR model. If it is too large, the spectrum will be distorted; too small, the improvement will be neglectable. The final result has to be adjusted by the practice.

5.3. Nonparametric mode-MUSIC algorithm

MUSIC (multiple-signal classification) is generally used in signal processing problems as a method for estimating the individual frequencies of multiple-harmonic signals [19–21]. The MUSIC algorithm makes use of the eigenvalue structure of the so-called multistatic response (MSR) matrix. A more detailed description of this algorithm can be found in [22]. It decompounds the eigenvector space of correlation matrices to signal space e_i and noise space V_k, because they are all orthogonal, their linear combinations are also orthogonal.

$$e_i^H\left(\sum_{k=M+1}^{p+1} a_k V_k\right)=0,\quad i=1,2\ldots M \tag{7}$$

Define $e\ (\omega)=[1,\ \exp(j\omega),.....,\exp(j\omega p)]^{\mathrm{T}}$, the spectrum power $\hat{P}_x(\omega)$ is shown as Eq. (8).

$$\hat{P}_x(\omega)=\frac{1}{\sum_{k=M+1}^{P+1} a_k|e^H(\omega)V_k|^2} \tag{8}$$

When $\omega=\omega_i$, $\hat{P}_x(\omega_i)$ should be infinite. But the error in correlation matrix estimation makes it have a finite value and a sharp peak. Because frequency of the peak acts as a sine signal, this could be made use of to reconstruct spectrum. The result proves it is even better than AR model. Substituting the definition $a_k=1(k=\mathrm{M}+1,\ldots,\ \mathrm{p}+1)$ in Eq. (8), the MUSIC spectrum power estimation is found to be

$$\hat{P}_{MUSIC}(\omega)=\frac{1}{e^H(\omega)\left(\sum_{k=M+1}^{P+1} V_k V_k^H\right)e(\omega)} \tag{9}$$

$M<p$ is the major scope of the MUSIC Algorithm application, where M is the sampling number and p is the dimension number of eigenvectors in signal space.

The MUSIC algorithm also implies the extrapolation of data and their autocorrelation functions just as most modern spectrum estimation, which would surly enhance the resolving power [20]. But the noise space makes it possible to reconstruct the spectrum approaching the real one mostly. Fig. 5 shows the reconstructed transmittance spectrum of the quasi-monochromatic light, which is obtained through MUSIC model, where there are few side lobes, the FWHM is only about 100 cm^{-1}, whose resolving power is more than double of the AR model's. It is totally perfect for spectrum reconstruction of quasi-monochromatic light and has extremely high signal-to-noise ratio. However, it should be recognized that the MUSIC model is very sensitive to the dimension number p, and it is not good at spectrum reconstruction of polychromatic light as monochromatic light.

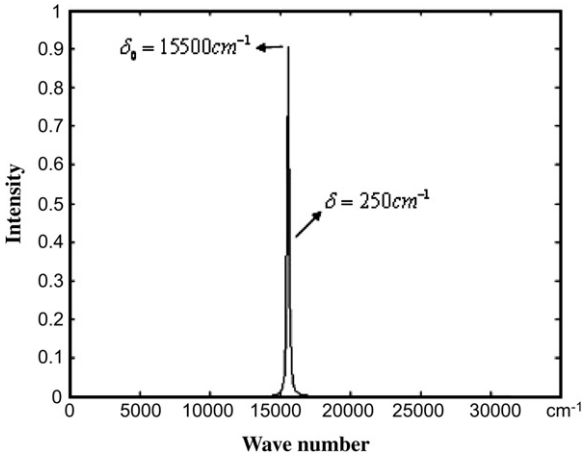

Fig. 4. Reconstructed transmittance spectrum of quasi-monochromatic light by AR Model.

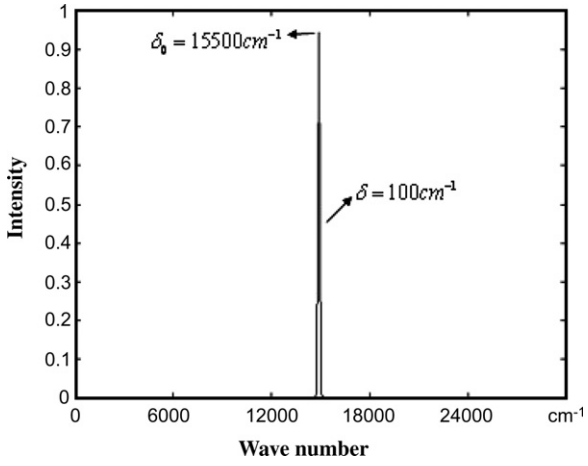

Fig. 5. Reconstructed transmittance spectrum of quasi-monochromatic light by MUSIC Model.

Table 1
The comparison of performances of different major algorithms

Algorithm	Time (point)/sec	Time (picture 800 × 600)/min	Resolving power/nm
Direct	15.811	158.11	20–50
FFT	0.016	0.16	20–50
AR	0.047	0.47	10–20
MUSIC	0.046	0.46	1–10

6. Conclusion

In actual work and study, not only the resolution power is important, but the time spent in data gathering and processing is also of concern [23–25]. Table 1 shows the time spent and spectrum quality of every algorithm using the same interferogram images shown in Fig. 2a.

Through comparing three different methods of spectrum reconstruction, it is obvious that the MUSIC Algorithm has a better power resolution than AR does. It is clearly indicated that the MUSIC Algorithm has tremendously improved the resolution of reproduced spectrum, and provided a better math model and the possibility of improvement for super advanced resolving power in spectrum reproduction. One attractive feature of the method is low cost: the entire investigation reported here used previously existing laboratory materials. The level of difficulty is perhaps slightly less than the skill and patience required for attainment and utilization of white light fringes from PIIS. In addition, although these methods are developed for PIIS, they are suitable for other style spectrometers, too. The only different work to do is to collect the interferential digital information by each modulation.

Acknowledgements

The authors gratefully acknowledge the support of Chinese National Natural Science Foundation and National High Technology Research and Development Program of China. This work is supported by the Key Program of National Natural Science Foundation of China (Grant No. 40537031); National High Technology Research and Development Program of China 863 (Grant No. 2006AA12Z152); National Defence Basic Scientific Research Project (Grant No. A1420080187); the National Natural Science Foundation of China (Grant No. 40375010; 60278019); the Science and Technology Plan Foundation of Shaanxi Province under Contract Nos. 2001K06-G12, 2005K04-G18; "985" Project of Xi'an Jiaotong University. Finally, we are thankful to Prof. Binxiang Li and Mr. Xinge Yan for their help with this paper.

References

[1] J.B. Rafert, R.G. sellar, J.H. Blatt, Appl. Opt. 34 (31) (1995) 7228.
[2] P.D. Matthew, A.K. Mohammad, Appl. Opt. 31 (28) (1992) 6096.
[3] L. John Otten III, Eugene W. Butler, SPIE 2480 (1995) 418.
[4] Chunmin Zhang, BaoChang Zhao, Bin Xiangli, Appl.Opt. 43 (33) (2004) 6090.
[5] Chunmin Zhang, Bin Xiangli, BaoChang Zhao, J. Opt. A: Pure Appl. Opt. 6 (8) (2004) 815.
[6] Chunmin Zhang, Bin Xiangli, BaoChang Zhao, Opt. Commun. 227 (4–6) (2003) 221.
[7] Chunmin Zhang, Bin Xiangli, BaoChang Zhao, Opt. Commun. 203 (1–2) (2002) 21.
[8] Chunmin Zhang, Bin Xiangli, BaoChang Zhao, SPIIS 4087 (2000) 957.
[9] Xiaohua Jian, Chunmin Zhang, BaoChang Zhao, ACTA Phys.Sin. 56 (2) (2007) 824.
[10] Chunmin Zhang, Baochang Zhao, Bin Xiangli, Optiks 117 (2006) 265.
[11] Chunmin Zhang, Jian He, Opt. Express 14 (26) (2006) 12561.
[12] Lei Wu, Chumin Zhang, Baochang Zhao, Opt. Commun. 273 (2007) 67.
[13] Robert John Bell, Introductory Fourier Transform Spectroscopy, Academic, New York, 1972.
[14] R. Glenn Sellar, Glenn D. Boreman, Laurel E. Kirkland, Proc. SPIE (2002) 389.
[15] Robert A. Neville, Lixin Sun, Proc. SPIE. (2003) 144.
[16] Robert A. Neville, Lixin Sun, Karl Staenz, Proc. SPIE. (2004) 208.
[17] M.A. Cutter, L.S. Johns, D.R. Lobb, T.L. Williams, Proc. SPIE. (2003) 392.
[18] Zhilin Yuan, Chunmin Zhang, Baochang Zhao, ACTA Phys. Sin. 56 (11) (2007) 6413.
[19] Ralph o. Schmidt, IEEE Trans. Antenn. Propag. 34 (3) (1986) 276.
[20] S.L. Wu, J.Q. Luo, Proc. IEEE (2006) 16.
[21] Habib Ammari, Ekaterina Iakovleva, Dominique Lesseler, SIAM J. Sci. Comput. (2005) 130.
[22] M. Cheney, Inverse Prob. 17 (2001) 591.
[23] Xiaohua Jian, Chunmin Zhang, Yao Sun, Baochang Zhao, ACTA Opt. Sin. 27 (4) (2007) 643.
[24] Zhihong Peng, Chunmin Zhang, Baochang Zhao, Yingcai Li, Fuquan Wu, Acta Phys. Sin. 55 (12) (2006) 6374.
[25] Jianyong Ye, Chunmin Zhang, Baochang Zhao, Acta Phys. Sin. 57 (1) (2007) 67.